JOURNAL OF SOLID STATE CHEMISTRY **122,** 214–220 (1996)
ARTICLE NO. 0104

Insertion of the Dinuclear Dihydroxo-Bridged Cr(III) Aquo Complex into the Layered Double Hydroxides of Hydrotalcite-Type

Norbert Gutmann[1] and Bernd Müller

Institut für Physikalische Chemie, Chemisch-Geowissenschaftliche Fakultät, Friedrich-Schiller-Universität Jena, D-07743 Jena, Germany

Received July 5, 1995; in revised form November 21, 1995; accepted December 5, 1995

A new hydrotalcite-like layered Cr–Zn double hydroxide (LDH), $[Zn_7Cr_4(OH)_{22}](CO_3)_2 \cdot 5H_2O$, was prepared by reaction of a perchlorate solution of the hydrolytic dimer $[(H_2O)_4Cr(\mu\text{-}OH)_2Cr(H_2O)_4]^{4+}$ with zinc oxide and subsequent anion exchange. The results of the studies by X-ray powder diffractometry, IR and UV–Vis spectroscopy, and thermal gravimetry were compared with the data of the known $[Zn_2Cr(OH)_6](CO_3)_{0.5} \cdot 1.5H_2O$ yielded by an analog reaction. Dissolving experiments show that the unchanged dimer and monomer units, respectively, are inserted into the hydroxide layers. Thereby the arrangement of the dimer units occurs in three possible domains with a parallel orientation to one another. Moreover, the parameters *a* and *c* of the hydrotalcite-like hexagonal lattice are decreased minimally. The strength of H bonding between OH groups and intercalated carbonate ions remains almost unchanged.

INTRODUCTION

Hydrotalcite-like layered double hydroxides (LDHs) have recently attracted growing interest: for instance, in the production of catalysts and catalyst carriers (1–4), as gas adsorbens (5), as anion exchangers (6–11), as medical antacid (e.g., Talcid from the company Bayer), and as ionic conductors (in particular as protonic conductor) (12–15). Especially the intercalation of polyoxo-metallate anions into LDHs leads to molecular sieve-like materials with catalytic oxydation properties (16–18).

With regard to the composition, LDHs can be described by the general formula

$$[M^{2+}_{1-x}M^{3+}_x(OH)_2]^{x+}[X^{z-}_{x/z} \cdot nH_2O]^{x-}$$

(M^{2+}, M^{3+} = divalent and trivalent metal ion, respectively, X^{z-} = z-valent anion). In these compounds the positively charged brucite-like main layers in which M^{2+} is partially replaced by M^{3+} alternate with negatively charged interlayers containing the anions and water molecules. The stacking of the hexagonal close-packed hydroxide layers (with $a \approx 0.31$ nm (19)) can occur with different symmetry (polymorphism). Frequently the rhombohedral sequence ($c = 3c_0$) is found in synthetic LDHs. By intercalation of tetrahedral anions a predominance of the hexagonal stacking sequence is assumed (14, 20, 21). A comprehensive survey about double layer structures has been given by Allmann (19) and Taylor (22).

The most frequent manner of LDH preparation is by coprecipitation. A great number of LDHs containing various combinations of M^{2+}, M^{3+}, and X^{z-} ions was obtained by coprecipitation in alkaline solution under different conditions (1, 6, 8, 19, 23). For the preparation of Cr(III) containing LDHs this method arises some difficulties (3, 23, 24). On the other hand, a LDH of the formula $[M_2Cr(OH)_6]X \cdot nH_2O$ ($M = Cu^{2+}, Zn^{2+}$, X = monovalent anion) can be synthesized by reaction of a Cr(III) salt solution with the corresponding divalent oxide MO (7, 12, 21). The substitutional inertness of the mononuclear aqua complex $[Cr(H_2O)_6]^{3+}$ (monomer)[2] is suggested to be an essential criterion for the precipitation of an almost stoichiometrical LDH. Moreover, the surface morphology of the applied oxide should not be underestimated as an important factor of an ordered growth of the hydroxide phase (25). A superstructure expected for the $[M_2Cr(OH)_6]^+$ layers cannot be proven by X-ray diffraction. Competing condensation reactions of the Cr^{3+} aqua ion can be excluded under such conditions. Consequently, there are only deprotonated and nondeprotonated Cr^{3+} monomers in the solution. Oligonuclear and polynuclear complexes of trivalent

[1] Present address: Department of Chemistry, Monash University, Wellington Road, Clayton, Victoria 3168, Australia.

[2] In the following, the $[Cr(H_2O)_6]^{3+}$ complex and its deprotonation products $[Cr(H_2O)_{6-x}(OH)_x]^{(3-x)+}$ are denoted as monomers and the dinuclear dihydroxo-bridged aquo complex $[(H_2O)_4Cr(\mu\text{-}OH)_2Cr(H_2O)_4]^{4+}$ and its deprotonation products $[(H_2O)_{4-x}(OH)_xCr(\mu\text{-}OH)_2Cr(H_2O)_{4-y}(OH)_y]^{(4-x-y)+}$ as dimers, respectively.

0022-4596/96 $18.00

metal ions, so-called isopolyoxocations, with appropriate structure and kinetic inertness and/or thermodynamic stability which can be formed by such hydrolysis reactions become a real hindrance to precipitate mixed M^{2+}–M^{3+} hydroxide phases. On the other hand, such polynuclear complexes will determine structure and composition of the mixed phases if they are incorporated as a whole (26).

In this paper we can show that a LDH with isolated inserted, integral dimer units, $[Zn_7Cr_4(OH)_{22}]^{4+}$ $X_4^- \cdot nH_2O$, is obtained if a solution of the dinuclear complex, $[(H_2O)_4Cr\ (\mu\text{-}OH)_2Cr(H_2O)_4]^{4+}$ (dimer), is used instead of the monomer solution for reaction with ZnO. The comparison of $[Zn_7Cr_4(OH)_{22}](CO_3)_2 \cdot 5H_2O$ with the already known $[Zn_2Cr(OH)_6](CO_3)_{0.5} \cdot 1.5H_2O$ refers to only minor structural differences.

EXPERIMENTAL

Materials. Stock solutions of $[Cr(H_2O)_6](ClO_4)_3$ were prepared and analyzed as described elsewhere (27). Solutions of dimer perchlorate, $[Cr_2(\mu\text{-}OH)_2(H_2O)_8](ClO_4)_4$, were prepared by O_2 oxidation of Cr(II) obtained by Zn amalgam reduction of Cr(III) stock solutions (28). The dimer was separated from small impurities of monomer and polymers by ion-exchange chromatography using the procedure described by Stünzi and Marty (27). Analytical reagent grade compounds were used for all preparations. Water was deionized and distilled before use.

Synthesis. In a typical preparation of $[Zn_7Cr_4(OH)_{22}](ClO_4)_4 \cdot nH_2O$ an aqueous solution of dimer perchlorate (100 ml, $[Cr]_{tot} \approx 0.04$ mol · liter^{-1}, $[H^+] \approx 0.01$ mol · liter^{-1}, $[NaClO_4] \approx 1$ mol · liter^{-1}) was added slowly during a period of 4 hr with stirring at 50°C to a suspension of 400 mg of ZnO in 10 ml water. The presence of perchlorate as the sodium salt and as perchloric acid in this solution can be explained by the separation conditions of ion chromatography (27). Additionally, under these pH conditions the hydrolytic polymerization of the dimer as well as its acid cleavage are strongly hindered (27, 29). The ClO_4^- ions also have proven to be a necessary component for the formation of the LDH. During the addition of the dimer solution pH $\approx$ 4.5 was reached. The greyish-blue precipitate was filtered off, repeatedly washed with water, and air dried. For exchanging ClO_4^- the solid was suspended in 1 *M* Na_2CO_3 solution and held at room temperature for 24 hr with occasional shaking. After removing the solution the solid was repeatedly suspended in a fresh one (24 hr, room temperature). Afterward it was filtered off, washed until being electrolyte-free, and air dried.

The chemical analysis yielded the sum formula $[Zn_7Cr_4(OH)_{22}](CO_3)_2 \cdot \sim 5H_2O$. The water content is slightly uncertain. For its estimation the space required by carbonate in the interlayer was also considered. The results in detail are Zn 36.43% (det.), 36.61% (calc.); Cr 16.03%, 16.64%; C 2.09%, 1.92%; H 2.98%, 2.58%. The mole fraction of Cr x, $x = Cr/(Zn + Cr)$, is 4/11.

Instrumentation. The metal contents were determined complexometrically for Zn^{2+} and photometrically as CrO_4^{2-} for Cr^{3+} preceded by a separation from hydrochloric acid on the strong basic anion exchanger Dowex-1 (30). The contents of carbon (carbonate) and hydrogen (OH groups and crystal water) was ascertained by C–H–N analysis.

The X-ray powder diffraction measurements were carried out using a URD 6 diffractometer (Freiberger Präzisionsmechanik) with a LiF monochromator and Mo$K\alpha$ radiation. The thermal gravimetric analysis (TG) was performed with a home-built optomagnetically compensating thermobalance (31). Samples were measured under a stream of argon (20 ml · hr^{-1}) at a heating rate of 5°C · min^{-1}. FTIR spectra were recorded on KBr pellets using an IRF 180 spectrometer (ZWG Berlin). For recording both UV–Vis solution and powder reflectance spectra, a Cary 5 spectrometer (Varian) was used. $BaSO_4$ white standard was used for the reflection measurements and the reflectances R were converted into the Kubelka–Munk function $f(R) = (1 - R)^2/2R$.

RESULTS AND DISCUSSION

Composition of $[Zn_7Cr_4(OH)_{22}](CO_3)_2 \cdot 5H_2O$

Due to the dropwise addition of the dimer its concentration in the reaction solution remained small enough to prevent polymerization reactions. For control a representative sample of $[Zn_7Cr_4(OH)_{22}](CO_3)_2 \cdot 5H_2O$ was dissolved in perchloric acid. The Cr^{3+} species in the solution could easily be identified as dimers by the UV–Vis solution spectrum. The ion-exchange chromatographical characterization (27) afforded 98.7% of dimer, 0.9% of monomer, and 0.4% of higher oligomers and polymers.

Analog studies were carried out with the known $[Zn_2Cr(OH)_6](CO_3)_{0.5} \cdot 1.5H_2O$. In contrast to the greenish-blue solution of the new compound, a blue-purple solution showing the typical electronic spectrum of the monomer solution was obtained. By means of ion-exchange chromatography 99.3% of monomer and 0.7% of oligomers and polymers were found. All results of these UV–Vis solution studies are given in detail in Table 1. As a result, the structural feature of the initial Cr^{3+} complex—either monomer or dimer—remains unchanged during the formation of the hydroxide phase and no considerable condensations among Cr^{3+} species took place. The resulting main layers can therefore be described as layers of hydroxochromate(III) ions, $[(OH)_4Cr(\mu\text{-}OH)_2Cr(OH)_4]^{4-}$ and $[Cr(OH)_6]^{3-}$, respectively, the holes of which are filled by Zn^{2+}. The overall reaction of the double hydroxide precipitation proceeds according to

TABLE 1
UV–Vis Solution Spectra of Acidified $[Zn_7Cr_4(OH)_{22}](CO_3)_2 \cdot 5H_2O$ and $[Zn_2Cr(OH)_6](CO_3)_{0.5} \cdot 1.5H_2O$ and for Comparison Those of the Hydrolytic Cr(III) Monomer and Dimer

	$[Zn_7Cr_4(OH)_{22}](CO_3)_2 \cdot 5H_2O$	$[Cr_2(OH)_2(H_2O)_8]^{4+}$ (27)	$[Zn_2Cr(OH)_6](CO_3)_{0.5} \cdot 1.5H_2O$	$[Cr(H_2O)_6]^{3+}$ (27)
$\lambda_{max,I}$[a]	416	417	408	408
ε_I[b]	22.5	20.4	16.0	15.5
$\lambda_{max,II}$[a]	581	582	575	575
ε_{II}[b]	18.2	17.4	13.6	13.2

[a] Wavelength in nm.
[b] Molar extinction coefficient in liter $\cdot$ mol^{-1} $\cdot$ cm^{-1}.

$$2[Cr_2(OH)_2(H_2O)_8]^{4+} + 9ZnO + 4ClO_4^- \rightarrow [Zn_7Cr_4(OH)_{22}](ClO_3)_4 \cdot nH_2O + 2Zn^{2+} + (7 - n)H_2O.$$

The ClO_4^- ions can be easily exchanged by other anions. The exchange might be complete already after a few hours. Carbonate affinity as known for hydrotalcite (19) could not be observed. However, intercalated carbonate ions are hardly exchangeable by other ions as known from the literature (8). An exchange becomes possible when working with dilute acids ($\sim$0.01 *N*) (32).

X-Ray Powder Diffraction Patterns

The X-ray powder diffraction patterns (Fig. 1) show the features typical for LDHs: relatively sharp (00l) reflections in the range of large *d* values (small angles 2ϑ, respectively, basal spacing $c_0 = 0.724$ nm) and a broadening of the (*hkl*) reflections in the range of small *d* values (large angles 2ϑ, respectively). Consequently, the stacking order of the brucite-like layers is relatively consistent in the *c* direction, but these layers can be twisted against another (turbostratic disorder). A quantity to estimate the disorder in stacking of the main layers is the integral half-width of the (006) reflection $B_{(006)}$ (33). This quantity includes the crystallite size along the [001] direction, but also the disorder within the interlayers. The $B_{(006)}$ amount of 0.48° (2ϑ) of $[Zn_7Cr_4(OH)_{22}](CO_3)_2 \cdot 5H_2O$ suggests a slightly higher degree of disorder compared to that of $[Zn_2Cr(OH)_6](CO_3)_{0.5} \cdot 1.5H_2O$ (0.34°).

The observed reflections could be indexed hexagonally like hydrotalcite with rhombohedral stacking sequence ($c = 3c_0$) (19, 20). Powder data and indexing of both compounds are shown in Table 2. Parameters *a* and *c* of the

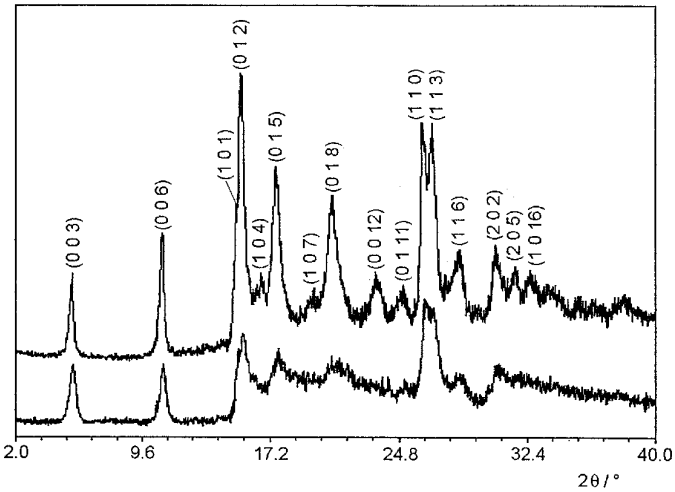

FIG. 1. Powder diffractograms of $[Zn_7Cr_4(OH)_{22}](CO_3)_2 \cdot 5H_2O$ (lower presentation) and $[Zn_2Cr(OH)_6](CO_3)_{0.5} \cdot 1.5H_2O$ (upper presentation) (Mo$K\alpha$ radiation).

TABLE 2
X-Ray Powder Patterns and Indexing of $[Zn_7Cr_4(OH)_{22}](CO_3)_2 \cdot 5H_2O$ with $a = 0.310_5$ nm and $c = 3c_0 = 2.265_4$ nm and $[Zn_2Cr(OH)_6](CO_3)_{0.5} \cdot 1.5H_2O$ with $a = 0.312_0$ nm and $c = 3c_0 = 2.274_7$ nm

	$[Zn_7Cr_4(OH)_{22}](CO_3)_2 \cdot 5H_2O$			$[Zn_2Cr(OH)_6](CO_3)_{0.5} \cdot 1.5H_2O$		
h k l	I/I_0	d_{exp} (nm)	d_{calc} (nm)	I/I_0	d_{exp} (nm)	d_{calc} (nm)
0 0 3	50	0.755	0.755	30	0.765	0.758
0 0 6	50	0.3780	0.3776	45	0.3808	0.3791
1 0 1	60	0.2668	0.2670	55	0.2678	0.2683
0 1 2	80	0.2623	0.2616	100	0.2630	0.2629
0 0 9	40	0.2521	0.2571			
1 0 4				25	0.2446	0.2440
0 1 5	60	0.2308	0.2312	70	0.2325	0.2323
1 0 7				15	0.2070	0.2077
0 1 8	55	0.1958	0.1950	55	0.1957	0.1959
0 0 12				25	0.1902	0.1896
1 0 10	35	0.1740	0.1733	20	0.1739	0.1740
0 1 11	35	0.1627	0.1635	15	0.1632	0.1642
1 1 0	100	0.1552	0.1552	75	0.1561	0.1560
1 1 3	95	0.1524	0.1521	75	0.1529	0.1528
1 1 6	35	0.1437	0.1436	30	0.1444	0.1443
2 0 2	45	0.1334	0.1335	30	0.1342	0.1342
2 0 5				20	0.1293	0.1295

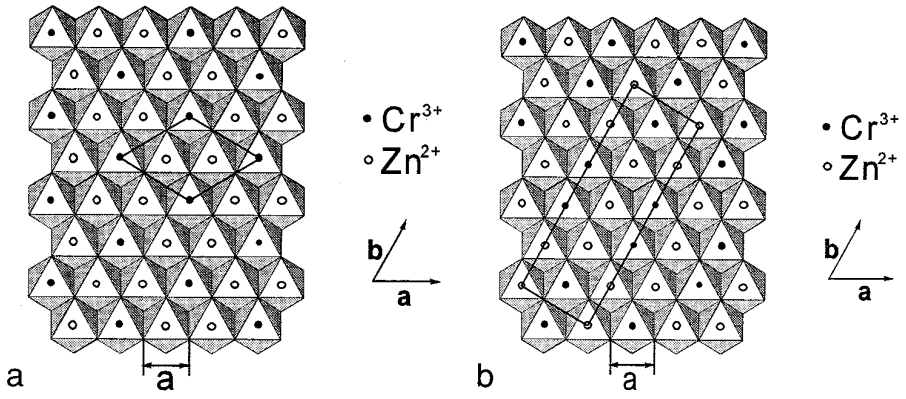

FIG. 2. Metal ion ordering in the brucite-like layers: (001) projection of the ordered octahedral sheet in (a) $[Zn_2Cr(OH)_6]^+$, showing the possible, but not proved supercell with $a' = \sqrt{3}\,a$, (b) $[Zn_7Cr_4(OH)_{22}]^{4+}$, showing one of the possible domains of parallel Cr–dimer orientation ([010] orientation) with an orthorhombic supercell ($a' = \sqrt{3}\,a$ and $b' = 5a$).

Cr-rich compound, $[Zn_7Cr_4(OH)_{22}](CO_3)_2 \cdot 5H_2O$, (0.310 and 2.265 nm, respectively) are slightly smaller than those of the Cr-poor one, $[Zn_2Cr(OH)_6](CO_3)_{0.5} \cdot 1.5H_2O$, (0.312 and 2.274 nm, respectively). The larger Cr content reduces not only parameter a but also c as a result of a more positive charge of the main layer (Vegard's law).

In the case of $[Zn_2Cr(OH)_6](CO_3)_{0.5} \cdot 1.5H_2O$ only the arrangement of Cr^{3+} and Zn^{2+} ions in the manner shown in Fig. 2a is possible although the resulting superlattice is not detectable. This arrangement is a requirement arising from the isolated Cr monomer insertion into the hydroxide phase and the Zn/Cr ratio. In the case of dimer insertion the highest ordered arrangement should be the parallel orientation of the Cr^{3+} pairs to each other as shown in Fig. 2b. However, the result of this is a Zn/Cr ratio of 3/2 ($x = 2/5$) and a nonhexagonal symmetry (rather a orthorhombic one, Fig. 2b). The experimentally found higher Zn content ($x = 4/11$) leads to the conclusion that domains of parallel dimer arrangements are more likely in the real lattice. Within such a domain one of the three statistical orientation possibilities should be dominant ([010], [100], and [110] orientations concerning the hexagonal OH close-packing). On the domain boundaries a statistical insertion of the octahedra pairs should occur. Then, however, only the minimum Cr content of $x = 1/4$ can be expected here. Considering the domain boundaries the total value of x must become smaller than the theoretical value of 2/5. The domains do not seem to be too large so that minimal deviations from the hexagonal metrics results. Consequently, a broadening of the reflections occurs, but no splitting. However, it remains uncertain to what extent possible disturbances caused by dimer insertion are involved in this broadening.

Data of Thermal Analyses

The results of thermal gravimetric analyses (TG and DTG) are shown in Fig. 3. The oxides Cr_2O_3 and ZnO, as well as mixed oxide phases including spinel phases, were assumed to be the end products of the thermal decomposition up to 700°C. The TG curve does not exhibit defined plateaus between the decomposition steps which extend over relatively high temperature ranges. This observation is in agreement with the well-known decomposition mechanism of such compounds which predicts two distinctive steps of weight loss (12, 34). The first reflects the loss of surface and crystal water; the second corresponds to the dehydroxylation and the removal of the anion. While the loss of surface water begins as soon as heating and is com-

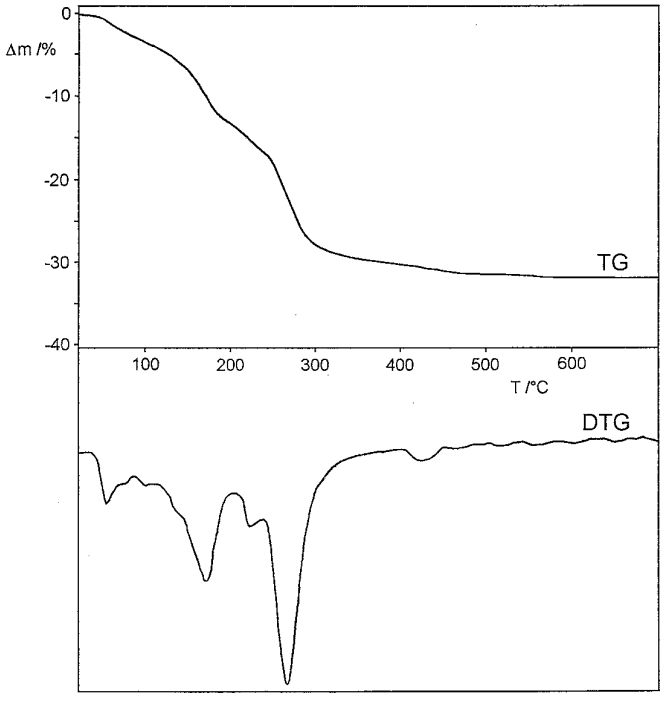

FIG. 3. TG and DTG curves of $[Zn_7Cr_4(OH)_{22}](CO_3)_2 \cdot 5H_2O$.

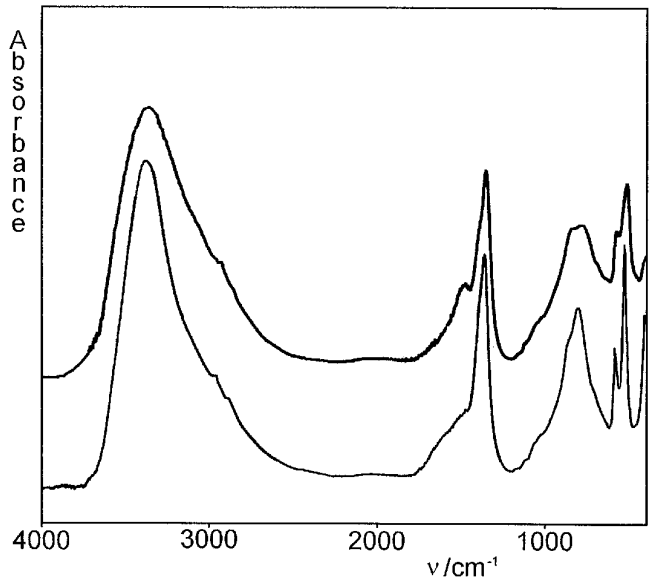

FIG. 4. IR absorption spectra of $[Zn_7Cr_4(OH)_{22}](CO_3)_2 \cdot 5H_2O$ (upper presentation) and $[Zn_2Cr(OH)_6](CO_3)_{0.5} \cdot 1.5H_2O$ (lower presentation).

plete at 90°C, the removal of the interlayer water is finished at 190°C. In the case of the second distinctive decomposition step the partial processes are more overlapped. This step starts as a partial dehydroxylation (12) causing the peak at 220°C in the DTG curve. At temperatures above 330°C the thermal decomposition is principally completed. Only kinetically hindered residual OH groups are decomposed (12).

IR Data

Figure 4 shows the IR spectrum of $[Zn_7Cr_4(OH)_{22}](CO_3)_2 \cdot 5H_2O$ compared with that of $[Zn_2Cr(OH)_6](CO_3)_{0.5} \cdot 1.5H_2O$. Despite of small differences, the bands of both spectra have approximately the same positions. The absorptions at 520 and 570 cm^{-1} and 520 and 580 cm^{-1}, respectively, can be assigned to metal–oxygen stretching vibrations (ν(CrO) and ν(ZnO)). The broad band at 3360 cm^{-1} is caused by stretching vibrations of H-bonded OH groups. Noteworthy is the long-wave position of this band in comparison to other LDHs of different M^{2+}–M^{3+} composition and anion intercalation (for comparison, see (5, 34, 35) and references therein). The H bonds formed here with the intercalated CO_3^{2-} ion are of higher strength. The slightly larger band width in the case of $[Zn_7Cr_4(OH)_{22}](CO_3)_2 \cdot 5H_2O$ could be caused by more distinctive OH groups. A O–H ··· O distance of 0.278 nm can be estimated for this interaction according to the correlations for H bonds given by Schwarzmann (36). Besides the geometry and the charge of the anion the H-bonding length is a factor which also determines the interlayer spacing. Surprisingly, the broad band at about 3100 cm^{-1} which is typical for H-bonding interaction between intercalated water and anion within carbonate containing LDHs (33, 34) cannot be detected. The bands of bending vibrations associated with the OH groups are in the range between 900 and 700 cm^{-1}. They are partially superimposed by bending vibrations of carbonate. The band at 1350 and 1360 cm^{-1}, respectively, can be assigned to the asymmetrical C–O stretching vibration of CO_3^{2-}. Its position is slightly shifted compared to that of the undisturbed ion (1410–1450 cm^{-1} (37)). This is probably due to the splitting of this transition since the D_{3h} symmetry of CO_3^{2-} decreases due to H bonding of CO_3^{2-} with OH groups and intercalated water. As a further consequence an additional transition appears quite clearly in the case of $[Zn_7Cr_4(OH)_{22}](CO_3)_2 \cdot 5H_2O$ as a band at 1480 cm^{-1}. Additionally, the symmetrical C–O stretching vibration becomes IR active resulting from the symmetry decrease (35). The absorptions in the range of about 1050 cm^{-1} should be assigned to this vibration. The positions of all observed bands caused by C–O vibrations agree well with the pattern of bands which is typical for polydentately interacting CO_3^{2-} (37).

UV–Vis Data

The powder reflectance spectra of both the studied compounds (Fig. 5 and Table 3) reveal two distinct bands indicating Cr^{3+} in a nearly octahedral OH^- environment. These bands are assigned to the transitions $^4A_{2g} \rightarrow {}^4T_{2g}$ and $^4A_{2g} \rightarrow {}^4T_{1g}(^4F)$. The spin-forbidden $^4A_{2g} \rightarrow {}^2E_g$ transition is to a certain extent evident only in the case of

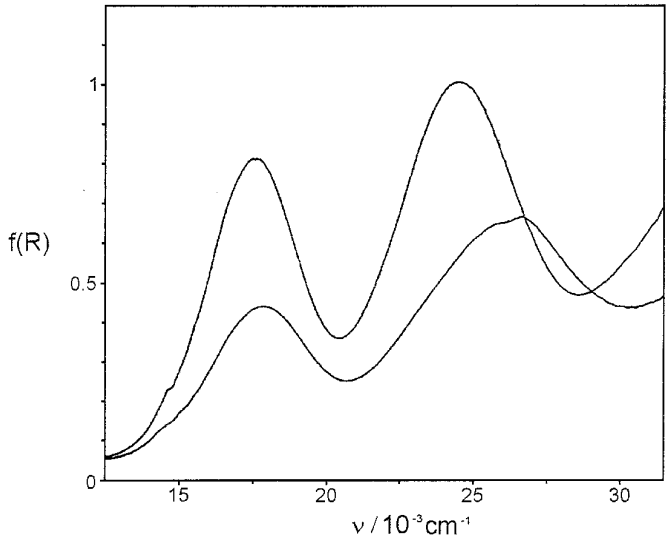

FIG. 5. UV–Vis powder reflectance spectra of $[Zn_7Cr_4(OH)_{22}](CO_3)_2 \cdot 5H_2O$ (upper presentation) and $[Zn_2Cr(OH)_6](CO_3)_{0.5} \cdot 1.5H_2O$ (lower presentation).

TABLE 3
Band Positions (in cm^{-1}) within the UV–Vis Powder Reflectance Spectra for $[Zn_2Cr(OH)_6](CO_3)_{0.5} \cdot 1.5H_2O$ and $[Zn_7Cr_4(OH)_{22}](CO_3)_2 \cdot 5H_2O$

$[Zn_2Cr(OH)_6](CO_3)_{0.5} \cdot 1.5H_2O$	$[Zn_2Cr_4(OH)_{22}](CO_3)_2 \cdot 5H_2O$	Assignment
26,600	24,500	$^4A_{2g} \rightarrow {}^4T_{1g}({}^4F)$
25,570		
17,900	17,480	$^4A_{2g} \rightarrow {}^4T_{2g}$
	14,700	$^4A_{2g} \rightarrow {}^2E_g$

$[Zn_7Cr_4(OH)_{22}](CO_3)_2 \cdot 5H_2O$. Similar positions for the two spin-allowed transitions have been found for the related Cr-containing minerals stichtite $[Mg_3Cr(OH)_8](CO_3)_{0.5} \cdot 2H_2O$ (38) and chromium chlorite[3] (other names for the latter mineral are kotschubeite, kämmerite, and clinochlore) (38, 39).

The actual microsymmetry of the Cr^{3+} ligand field is however trigonal (point group D_{3d}) caused by two different average OH–OH distances, 0.273 and 0.311 nm (19). As a result, a $Cr(OH)_6$ coordination octahedra is compressed along the threefold main axis of rotation. The consequence of the symmetry lowering is a splitting of the $^4T_{2g}$ and $^4T_{1g}$ terms each into the following terms ^4E and $^4A_1$ (40, 41). In the present cases considerable band broadening is observed mainly for the higher energy band. For $[Zn_2Cr(OH)_6](CO_3)_{0.5} \cdot 1.5H_2O$ this band has the shape of a double peak. Analogous spectral features were also found, for example, for Cr^{3+} incorporated spinel compounds in which the lattice places occupied by Cr^{3+} have the same D_{3d} symmetry (42–45). Based on the results of these investigations both a slight widening of the Cr–OH bonds and a greater polarization of the OH groups due to the slightly increased part of trivalent Cr^{3+} ions might be considered as possible reasons for a shift of the two transitions toward lower wavenumbers. Both effects give rise to a band shift into the same direction (42–45).

CONCLUSIONS

The dinuclear $[(H_2O)_4Cr(\mu\text{-}OH)_2Cr(H_2O)_4]^{4+}$ complex was inserted separately as an integral unit into the hydroxide layers of a hydrotalcite-like structure with the formula $[Zn_7Cr_4(OH)_{22}](CO_3)_2 \cdot 5H_2O$ by reaction of the corresponding aqueous solution with ZnO. In contrast, the analogous and well-known reaction of the mononuclear $[Cr(H_2O)_6]^{3+}$ complex leads to a LDH with unlinked Cr^{3+} centers within the hydroxide layer. The resulting structural changes in the new LDH compared to that yielded by using the monomer are minimal: slight diminution of the parameters a and c of the hydrotalcite-like lattice, nearly the same H bond lengths between main layer OH groups, and interlayer carbonate ions.

[3] According to Bish (39) the Cr^{3+} ions are only located within the positively charged Al–Mg hydroxide layers under partial replacement of Al^{3+} ions, but not within the negatively charged mica layers.

ACKNOWLEDGMENT

We thank Professor Allmann for very helpful discussions.

REFERENCES

1. O. Clause, B. Rebours, E. Merlen, F. Trifiro, and A. Vaccari, *J. Catal.* **133,** 231 (1992).
2. T. Kwon, G. A. Tsigdinos, and T. J. Pinnavaia, *J. Am. Chem. Soc.* **110,** 3653 (1988).
3. W. T. Reichle, *J. Catal.* **94,** 547 (1985).
4. J. G. Nunan, P. B. Himelfarb, R. G. Herman, K. Klier, C. E. Bogdan, and G. W. Simmons, *Inorg. Chem.* **28,** 3868 (1989).
5. S. Miyata and T. Hirose, *Clays Clay Miner.* **26,** 441 (1978).
6. S. Miyata and T. Kumura, *Chem. Lett.* 843 (1973).
7. H. P. Boehm, I. Steinle, and C. Vieweger, *Angew. Chem.* **89,** 259 (1977).
8. A. Mendiboure and R. Schöllhorn, *Rev. Chim. Miner.* **23,** 819 (1986).
9. H. Koppka, K. Beneke, and G. Lagaly, *J. Colloid Interface Sci.* **123,** 427 (1988).
10. M. Meyn, K. Beneke, and G. Lagaly, *Inorg. Chem.* **29,** 5201 (1990).
11. A. Ookubo, K. Ooi, F. Tani, and H. Hanyashi, *Langmuir* **10,** 407 (1994).
12. M. Lal and A. T. Howe, *J. Solid State Chem.* **39,** 368 and 377 (1981).
13. A. de Roy and J. P. Besse, *Solid State Ionics* **35,** 35 (1989).
14. A. de Roy and J. P. Besse, *Solid State Ionics* **46,** 95 (1991).
15. R. Oesten and H. Böhm, *Solid State Ionics* **62,** 199 (1993).
16. M. A. Drezdzon, *Inorg. Chem.* **27,** 4628 (1988).
17. E. D. Dimotakis and T. J. Pinnavaia, *Inorg. Chem.* **29,** 2393 (1990).
18. R. S. Weber, P. Gallezot, F. Lefebvre, and S. L. Suib, *Micropor. Mater.* **1,** 223 (1993).
19. R. Allmann, *Chimia* **24,** 99 (1970).
20. K. El Malki, A. de Roy, and J. P. Besse, *Eur. J. Solid State Inorg. Chem.* **26,** 339 (1989).
21. K. El Malki, M. Guenane, C. Forano, A. de Roy, and J. P. Besse, *Mater. Sci. Forum* **91–93,** 171 (1992).
22. H. F. W. Taylor, *Mineral. Mag.* **39,** 377 (1973).
23. W. T. Reichle, *Solid State Ionics* **22,** 135 (1986).
24. R. P. Grosso, Jr., S. L. Suib, R. S. Weber, and P. F. Schubert, *Chem. Mater.* **4,** 922 (1992).
25. N. Gutmann and B. Müller, in preparation.
26. O. P. Krivorutshko, N. A. Pakhamov, L. M. Plyasova, S. V. Ketshik, R. A. Buyanov, and G. R. Kotel'nikov, *Kinet. Katal.* **24,** 200 (1983).

27. H. Stünzi and W. Marty, *Inorg. Chem.* **22,** 2145 (1983).
28. M. Ardon and G. Stein, *J. Chem. Soc.* 2095 (1956).
29. F. P. Rotzinger, H. Stünzi, and W. Marty, *Inorg. Chem.* **25,** 489 (1986).
30. N. Gutmann, B. Müller, and H.-J. Tiller, *J. Solid State Chem.* in press.
31. W. Ludwig, J. Opfermann, and G. Wilke, Wiss. Beitr. Friedrich-Schiller-Univ. Jena, Therm. Analysenverfahren in Industrie und Forschung **2,** 159 (1983).
32. D. L. Bish, *Bull. Mineral.* **103,** 170 (1980).
33. E. Ivana, R. Marchidan, and R. Mănăila, *Bull. Soc. Chim. Belg.* **101,** 101 (1992).
34. E. C. Kruissink, L. L. van Reijen, and J. R. H. Ross, *J. Chem. Soc., Faraday Trans. I* **77,** 649 (1981).
35. M. J. H. Hernandez-Morena, M. A. Ulibarri, J. L. Rendon, and C. J. Serna, *Phys. Chem. Mineral.* **12,** 34 (1985).
36. E. Schwarzmann, *Z. Anorg. Allg. Chem.* **317,** 176 (1962).
37. G. Busca and V. Lorenzelli, *Mater. Chem.* **7,** 82 (1982) and references therein.
38. G. Calas, A. Manceau, A. Novikoff, and H. Boukili, *Bull. Minéral.* **107,** 755 (1984).
39. D. L. Bish, *Am. Mineral.* **62,** 385 (1977).
40. D. Reinen, *Struct. Bond.* **6,** 30 (1969).
41. C. P. Poole, Jr. and J. F. Itzel, Jr., *J. Chem. Phys.* **39,** 3445 (1963).
42. D. L. Wood, G. F. Imbusch, R. M. Macfarlane, P. Kisluik, and D. M. Larkin, *J. Chem. Phys.* **48,** 5255 (1968).
43. O. Schmitz-Du Mont and D. Reinen, *Z. Elektrochem.* **63,** 978 (1959).
44. D. Reinen and O. Schmitz-Du Mont, *Z. Anorg. Allg. Chem.* **312,** 121 (1961).
45. J. S. Reed, *J. Am. Ceram. Soc.* **54,** 202 (1971).